2013 IEEE International Conference on Robotics and Automation (ICRA)
Karlsruhe, Germany, May 6-10, 2013

An Experimental Robotic Testbed for Accelerated Development of Ankle Prostheses

Joshua M. Caputo and Steven H. Collins
Department of Mechanical Engineering, Robotics Institute
Carnegie Mellon University, Pittsburgh, Pennsylvania 15213-3815
biomechatronics.cit.cmu.edu, stevecollins@cmu.edu

***Abstract*—Biomechatronic devices show promise for restoring human performance, but development has been made inefficient by the need for specialized autonomous devices prior to testing benefits of proposed functionalities. This has severely limited exploration within and across intervention strategies. We have developed a laboratory testbed suitable for emulating and rapidly assessing wearable robot designs. The testbed is comprised of powerful off-board motor and control hardware, a flexible tether, and lightweight instrumented end-effectors worn by a person. We performed a series of benchtop tests to gauge mechatronic performance, and found significant improvements over prior candidate testbed platforms. In particular, this system has an unusual combination of low worn mass (less than 1 kg), high closed-loop torque bandwidth (17 Hz), and high peak torque (175 N·m), key to emulating specialized devices. We also performed walking trials to gauge dynamic torque control and versatility. Walking trials with a prosthesis end-effector demonstrated precise torque tracking (4 N·m RMS error), both in time and joint-angle space, and versatile mechanical behavior through systematic changes in high-level control law parameters. For example, we widely varied net ankle work (from -3 J to 9 J per step) using an impedance law relating joint angle and velocity to desired torque. These results suggest such testbeds could be used to emulate and evaluate novel assistive robot concepts prior to laborious product design.**

I. Introduction

Advanced prosthetic technologies could improve quality of life for individuals with lower-limb amputation, which affects 1.6 million (5 in 1,000) people in the United States [1]. Conventional prostheses limit locomotion performance and mobility for users by several functional measures, including metabolic energy cost and preferred walking speed [2, 3].

Robotic devices capable of active control show promise for improving locomotor performance [4–10]. For example, Herr and Grabowski [11] recently demonstrated the first robotic ankle to significantly reduce energy cost for amputees.

Such results have been achieved despite very limited exploration of possible prosthesis *functionalities*. Current development approaches require years of design and refinement before an assistance strategy can be evaluated by human users [e.g. 4–7]. Autonomy presents the greatest design challenge, leading to specialized devices with limited utility as experimental tools and narrow resulting findings. Our field has spent too much effort learning *how* to implement various functionalities and not enough learning *which* ones would benefit users.

Laboratory testbeds, by contrast, have often been used as versatile exploratory tools in basic research on, e.g., human neuromechanics [12, 13]. Such systems typically serve as probes, requiring only moderate mechatronic performance to gain useful insights. With improved fidelity, perhaps such tools could be used to emulate specialized, wearable robots [14].

We have developed a high-performance testbed intended to accelerate the development process for robotic ankle-foot prostheses. This tool leverages the advantages of a laboratory setting, using tethered off-board motor and control components to achieve high performance with a simple design. Only one drive and tether is needed for a variety of end-effectors, which are lightweight to minimize interference with natural motions. Precise control of human-robot interaction torques allow emulation of common mechanical design elements. Torque control prevents interactions being dominated by robot position, which can restrict human engagement [15]. We chose the ankle for its commonality to lower-limb disabilities [3] and mechanical importance in locomotion [16]. Here we report the platform's fundamental capabilities and the results of demonstrative locomotion trials in which we systematically varied ankle push-off work. This test serves as an example of a potential use of such systems in the design process; increased work could reduce human energy cost [7, 12], but requires larger, heavier motors and batteries, or shorter range, in autonomous devices, so delineating the trade-off informs autonomous designs for target patient groups.

II. Methods

We designed and constructed an experimental robotic ankle testbed with a prosthetic end-effector, implemented plantarflexion torque control at the ankle, and measured system performance in a series of benchtop and walking tests.

A. Mechatronic Design

The electromechanical system comprises a powerful off-board motor and control system, a flexible tether, and an instrumented prosthesis (Figure 1). We used a high-torque, low-inertia electrical motor and drive with embedded velocity control (1.61 kW AC servomotor, Baldor Electric Corp.). Desired motor velocity commands were generated using a high-speed, real-time control module (ACE1103, dSPACE Inc.) at 500 Hz. Mechanical loads and displacements were transmitted between the motor and end-effector with a flexible Bowden cable measuring 3.5 m in length and comprising a flexible coiled steel outer conduit (415310-00, Lexco Cable Mfg.) and a 3 mm synthetic inner rope (Vectran Fiber Inc.).

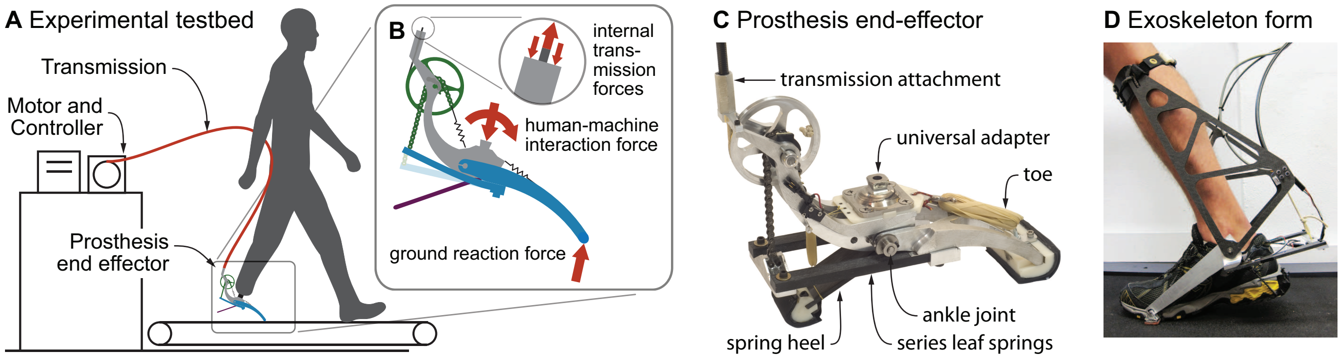

Fig. 1. Mechatronic design. **A.** The experimental testbed comprises: (1) powerful off-board motor and control hardware, (2) a flexible tether transmitting mechanical power and sensor signals, and (3) a lightweight instrumented end-effector. This division of components was chosen to maximize responsiveness and minimize end-effector mass. **B.** Free-body diagram of the end effector. Bowden cable tether forces are transmitted through a leaf spring to the toe, giving rise to ankle plantarflexion torques. **C.** Photograph of the instrumented prosthesis. A universal adapter attaches to the pylon or prosthesis simulator boot worn by the user. Fiberglass leaf springs provide series elasticity for ankle torque measurement and control. **D.** Photograph of an alternate exoskeleton end-effector.

We designed an instrumented prosthesis (Figure 1C) to convert transmission forces into ankle plantarflexion torques and to measure joint configuration and torques. Transmission forces pull on a series spring connected to the toe, generating plantarflexion moments (Figure 1B) similar to the action of the Achilles tendon in biological ankles. These springs decouple motor inertia from the toe segment, which can improve torque tracking during, e.g., intermittent ground contact [17, 18]. A low-tension spring pulled the toe upwards when transmission forces were low. We attached a compliant heel spring to the frame. This designs was constructed using custom and catalog components chosen for low mass and durability.

B. Sensing and control

We directly measured ankle position and torque, and used low-level proportional control to maintain desired torques. We also implemented several torque-limiting safety features.

We measured ankle torque using calibrated models of spring deflection. We performed calibration trials in which the end-effector was fixed while known masses were hung from the toe, then fit model coefficients using least squares regression.

We used proportional control of motor velocity to maintain desired ankle torque. We applied the low-level command: $\omega_m = K_p \cdot (\tau_d - \tau)$, where ω_m is the velocity commanded to the motor driver, K_p is the proportional gain, and τ_d and τ are desired and measured ankle torque, respectively. K_p was determined from a mathematical model, then hand tuned. We used a similar function to perform ankle position control during the swing phase of walking by substituting a position error for torque error and using a modified gain.

We designed several safety features, in both software and hardware, to limit forces exerted on the user. We placed software limits on the maximum desired torque and motor velocity, and provided user and experimenter with electrical disable switches. We also included a mechanical break-away in the transmission, and empirically verified breaking tension.

C. Benchtop testing methods

We conducted benchtop tests characterizing device performance in terms of torque measurement accuracy, peak torque, peak power, closed-loop torque step response, closed-loop torque bandwidth, and tether interference. These tests were designed to reveal fundamental aspects of system performance and to allow comparison with existing platforms.

We first evaluated the accuracy of our calibrated torque measurement. We applied a range of known ankle torques using static loading with free weights. We applied a variety of loads in a variety of joint configurations, and compared measured and applied torques. We computed the root mean square (RMS) error and the maximum absolute error.

We performed step response tests with a fixed joint to characterize closed-loop torque response time and demonstrate peak torque capacity. During these trials, we rigidly fixed the prosthesis frame and toe to the benchtop, locking the ankle joint, and programmed desired torque as a square wave with a magnitude of 175 N·m. We tuned K_p so as to minimize rise time with zero overshoot. We collected data for 10 complete cycles, averaged the measured torque trajectories, and computed 90% rise and fall times.

We performed similar step response tests with a compliant load to demonstrate peak power. During these trials, we rigidly fixed the prosthesis frame to the benchtop and attached the toe to the benchtop through a coil spring with stiffness of 26,000 N·m^{-1}. Desired torque was programmed as a square wave in time. We collected data for 10 complete cycles, averaged the computed power trajectories, and computed peak power as the maximum of the average power trajectory.

We characterized closed-loop torque control bandwidth using frequency-domain transforms of the system's response to a chirp in desired torque. During bandwidth trials, we rigidly fixed the prosthesis frame and toe to the benchtop, locking the ankle joint and programmed desired torque as an offset chirp oscillating between 50 and 110 N·m at frequencies rising from 0 to 30 Hz. We tuned K_p to maximize bandwidth with minimal resonance. We mathematically approximated both input (desired torque) and output (measured torque) signals in the frequency domain using a fast Fourier transform (FFT) and used these to calculate magnitude and phase response. We collected data for 10 trials, smoothed each resulting Bode

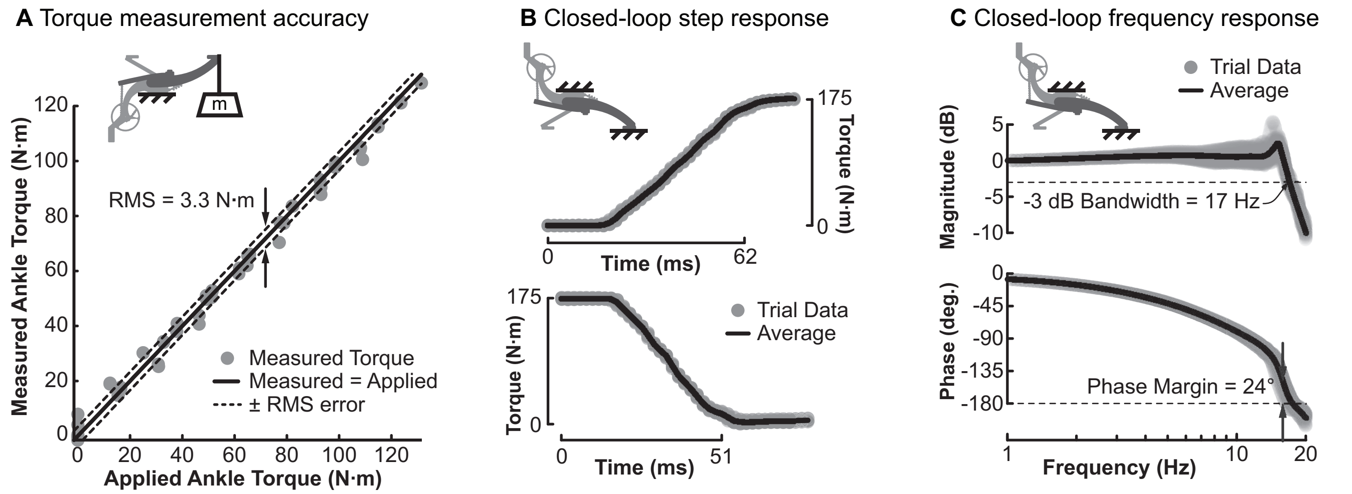

Fig. 2. Benchtop results. **A.** Torque measurement accuracy. We found RMS measurement error of 3.3 N·m and maximum error of 7.9 N·m. **B.** Closed-loop torque step response. We fixed the base and toe of the prosthesis and applied 175 N·m step changes in desired torque. Across 10 trials, we measured average 90% rise times of 0.062 s for steps up, fall times of 0.051 s for steps down, and 0% overshoot. **C.** Bode plot of frequency response under closed-loop torque control. We fixed the base and toe of the prosthesis and applied 50 N·m amplitude chirps in desired torque, then smoothed the resulting curves and averaged over 10 trials. We calculated an average -3 dB bandwidth of 17 Hz and an average phase margin of 23.6° .

plot (to remove FFT artifacts), averaged across trials, and calculated -3 dB bandwidth and 0 dB phase margin.

We performed experiments with an anthropomorphic pendulum leg to characterize tether interference with natural motions. For controlled tests, we constructed a single-link pendulum with mass properties of a 50^{th} percentile male leg [19]. We attached the prosthesis to this leg and performed trials under two conditions: tether attached and tether removed. For each trial, we initialized the pendulum angle, allowed it to swing freely, and recorded the angle trajectory in time. We conducted 10 trials and calculated the stiffness and damping coefficient attributed to tether forces using a linear model.

D. Human walking testing methods

We designed a high-level impedance control law suitable for prosthesis walking demonstrations and performed tests to evaluate torque tracking performance and system versatility. A high-level impedance control law was used to calculate desired prosthesis torque based on ankle angle and gait cycle phase. We used the piecewise linear function in Figure 3A:

$$\tau_d = f(\theta, \phi) = k(\phi, \theta) \cdot (\theta - \theta_0(\phi, \theta)) \quad (1)$$

where τ_d is desired ankle torque, θ is ankle joint angle, ϕ is discrete gait phase, and k and θ_0 are stiffness and angle offset terms, respectively, that remain constant during each phase and over a range of joint angles. A finite-state machine advanced ϕ through three phases: *dorsiflexion*, during the beginning of stance; *plantarflexion*, during the end of stance; and *swing*. During each of the stance phases the ankle joint behaved as a stiffening spring comprised of two linear stiffness regions. Different values of k and θ_0 during plantarflexion phases enabled control of the net work produced or absorbed over the course of a step cycle. We chose default values such that the overall curve approximated the relationship observed for the human ankle during normal walking. We determined alternate parameters for a range of values of net ankle work. During the swing phase, the ankle was positioned for the next step.

We used a configuration prediction term to improve tracking of desired prosthesis torques during impedance control. We measured a lag of about 16 ms between commanded and observed motor velocity changes, which caused torque error during fast ankle motions. We modified the angle used in Eq. 1 to account for expected changes using:

$$\theta_p = \theta + t_{pred} \cdot \dot{\theta} \quad (2)$$

where θ_p is the predicted ankle angle substituted for θ, t_{pred} is a lag time constant, and $\dot{\theta}$ is the ankle velocity. This adjustment was based on a simplified model of system dynamics, and resulted in improved torque tracking.

We performed walking tests to evaluate testbed performance and versatility under realistic operating conditions. In all trials, one able-bodied subject (male, 84 kg, 1.85 m tall, 0.92 m leg length) walked on a treadmill at 1.25 m·s^{-1} for 10 minutes. The instrumented prosthesis was worn with a simulator boot on one leg [a well-established technique described in 7, 20, 21], and impedance control laws with five condition-specific plantarflexion parameters were applied. Data from the final minutes of each trial were captured and normalized to percent stance (scaled time), and we calculated RMS error between desired and measured torque and the average and standard deviation of net ankle work per step.

III. Results

The prosthesis end-effector had a mass of 0.96 kg and ankle joint range of motion of 14° (17°) in dorsiflexion to 35° (27°) in plantarflexion when unloaded (maximally loaded). Torque measurement errors were always less than 7.9 N·m, with RMS error of 3.3 N·m (or 1.9% of maximum torque, Figure 2A). Peak operating torque was at least 175 N·m (Figure 2B).

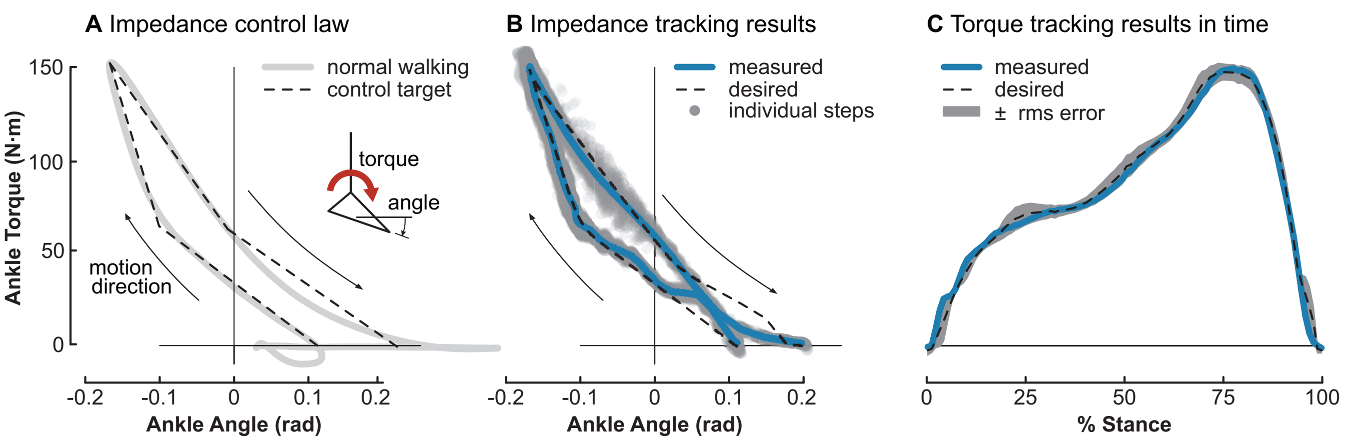

Fig. 3. Prosthesis impedance control during walking. **A.** Impedance control law. Desired torque is a piecewise linear function of ankle position, with separate dorsiflexion (negative velocity) and plantarflexion (positive velocity) phases. Default curve parameters approximate the relationship observed during normal walking. **B.** Measured torque-angle relationship during 6 minutes (270 steps) of walking at 1.25 m·s^{-1}. Each step resulted in a similar amount of net joint work, 4.67 ± 0.87 J. **C.** Joint torque over the stance period, normalized to % stance. Average stance duration was 0.83 ± 0.01 s, and average RMS torque error was 3.7 N·m. Note that time-trajectory error appears smaller than angle-torque error, while the latter is more meaningful in terms of work production.

We measured peak prosthetic ankle power of 1006 ± 20 W (avg. ± st. dev.), at a torque of 144 ± 1 N·m and velocity of 7.2 ± 0.3 rad·s^{-1}. At the instant of peak power, the series spring was being stretched (absorbing energy).

We measured a closed-loop prosthetic ankle torque step response rise time (90% of final value) of 0.062 ± 0.001 s (Figure 2B). We calculated a closed-loop ankle torque bandwidth (-3 dB magnitude criteria) of 17.1 ± 0.2 Hz and phase margin of 23.6 ± 5.3° (Figure 2C).

In experiments with an anthropomorphic pendulum leg, we characterized tether interference with a rotational stiffness about the hip joint, k_t, and rotational damping about the hip joint, b_t. Under maximum cable tension, we found negligible stiffness (k_t = -0.11 ± 0.62 N·m·rad^{-1}) and very little damping (b_t = 0.051 ± 0.003 N·m·(rad·s^{-1})$^{-1}$). For comparison, the untethered damping coefficient, from ball bearings and air resistance, was b_0 = 0.046 ± 0.001 N·m·(rad·s^{-1})$^{-1}$.

During walking trials with the prosthesis end-effector, we found tight correlation between desired and measured torque for a variety of control laws. Nominal RMS torque error was 3.7 N·m (Figure 3C), while net ankle work was 4.7 ± 0.9 J, with an error from desired of -2.5 ± 0.2 J (Figure 3B). Stance duration was 0.83 ± 0.01 s, and stride period was 1.34 ± 0.02 s. In trials with systematic variations in the control law (Figure 4), we measured net ankle joint work values of -3.3 ± 0.8, 0.2 ± 1.1, 4.7 ± 0.9, 7.2 ± 1.0, and 8.8 ± 1.7 J.

IV. Discussion

We developed an experimental platform for use in early-stage assessment of robotic ankle-foot prosthesis design concepts and conducted tests of the system's mechatronic performance. Walking trials demonstrated precise torque tracking, both in time and joint-angle space, and versatile mechanical behavior through systematic changes in high-level control law parameters. Benchtop tests revealed superior performance compared to prior torque-controlled devices, particularly in terms of worn mass and torque bandwidth. Our results suggest testbeds like this could be used to emulate novel robotic ankle design concepts and rapidly evaluate human response.

Pilot tests of walking with the robotic prosthesis testbed demonstrated the suitability of this experimental tool for emulating a wide variety of proposed device functions under realistic conditions. We measured very low torque tracking errors (Figure 3), and found that net work production could be systematically and consistently altered across conditions (Figure 4). Net prosthesis energy contributions are strongly tied to human performance [7, 11], and affect key device design requirements, such as motor and battery size. Consistent work production is challenging in torque-controlled actuator systems, however, because small changes in relative timing can result in significant changes in mechanical power. We demonstrated this system's capacity to systematically and repeatably manipulate the torque-displacement relationship, leading to a range of overall ankle behaviors consistent with damped springs, passive springs, human ankle musculature, or over-powered robotic prostheses. Dynamic consistencies were not due to fixed structural features which would limit versatility. The testbed can therefore emulate prosthesis designs with a wide range of mechanical features hypothesized to be beneficial, and alter these features online.

The exceptional versatility observed during walking trials was enabled by improved mechatronic performance compared to prior torque-capable designs, particularly in terms of worn mass and closed-loop torque bandwidth. High closed-loop torque bandwidth is important for dynamic emulation during periods of rapidly-changing conditions, such as the initial contact of the foot with the ground [22], while low mass is needed to avoid affecting natural limb motions or increasing user effort [23]. The prosthesis end-effector had lower mass than the lightest reported designs (0.96 kg vs. 1.37 kg in [24]), yet an order of magnitude greater bandwidth. Benchtop tests revealed higher closed-loop torque bandwidth than the highest open-loop bandwidth values reported for prior designs (17 Hz vs. 14 Hz in [4]), but with less than half the mass. The

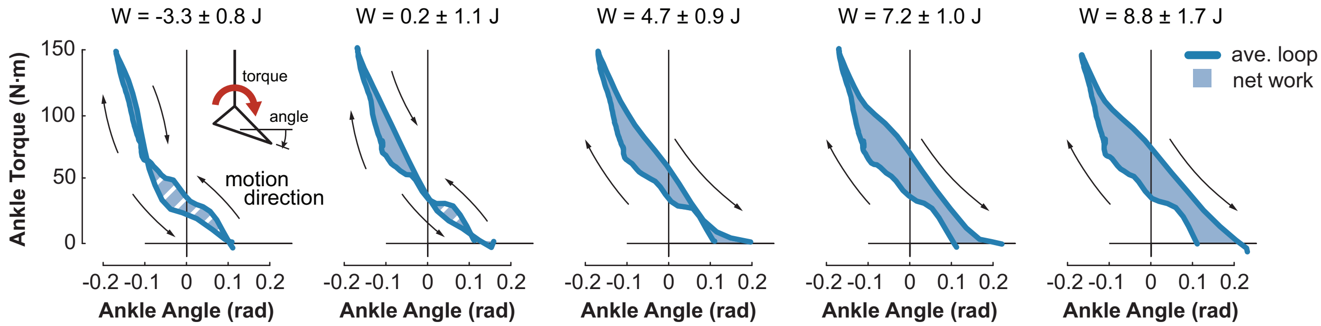

Fig. 4. Systematic modulation of net ankle work. We measured average net work per step as subjects walked at 1.25 m·s^{-1} for 6 minutes (270 steps) with plantarflexion control law parameters set to five different values. The testbed emulated a versatile range of behaviors, from damping consistent with conventional passive prostheses to nearly double the push-off work typically produced by the human ankle.

testbed exhibited higher peak torque (175 N·m vs. 134 N·m in [4]) and peak power (1006 W vs. 270 W in [25]) than prior experimental results. These results also compare well with observations of the human ankle and foot. We demonstrated peak torques 50% greater than those observed during human walking (1.6 N·m·kg^{-1} [16]), device mass less than a human foot (1.5% body mass [19]), and torque bandwidth twice that of ankle muscles (6-10 Hz [26]). Some other actuators have demonstrated similar torque bandwidth, but with substantially lower peak torque and greater mass [e.g. 27–30]. Improved performance was simply due to appropriate selection and distribution of components for this domain.

The primary feature allowing for improved mechatronic performance in this testbed was a Bowden-cable tether separating end-effectors from driving hardware. This division of components allowed the use of a powerful but heavy motor (1.61 kW, 10 kg) without additional mass worn by the user. Hydraulic or pneumatic tethers could allow a similar partition, but tend to result in higher worn mass or lower bandwidth. Tether forces could potentially interfere with user motions, but did not seem to do so in this case. We estimate tether torque about the hip joint was 0.4% of the peak torque produced by hip muscles. By contrast, an additional 2 kg in end-effector mass due to a small actuator [e.g. 31] would increase peak hip torque by about 4.6 N·m, or 17% [23] and metabolic cost by up to 44% [21]. Losses due to cable friction were of little relevance [32], since the highly over-powered motor acts mostly against its own inertia and ankle torques were measured on the end-effector side of the transmission. In a laboratory setting, replacing on-board hardware with a Bowden cable tethered to more capable off-board hardware seems to be advantageous both in terms of increased versatility and decreased interference with natural human motions.

Fiberglass leaf springs also contributed to low end-effector mass and low-error torque tracking. Physical series elasticity appeared to reduce torque errors at instants of large position disturbance, such as at initial toe contact (Figure 3A). Series elasticity has often been provided with steel coil springs in compression [27, 31] or torsion [29]. Fiberglass is eight times lighter than spring steel for a given strain energy capacity ($\rho{\cdot}E{\cdot}\sigma_y^{-2}$). This benefit can be offset somewhat by spring geometry in some cases, but in the case of torque production leaf springs can double as implicit levers, eliminating overall mass differences arising from spring geometry. The use of fiberglass leaf springs can therefore reduce spring mass by nearly 90% compared to steel springs, and saved an estimated 0.64 kg in this application.

Of course, numerous aspects of the testbed system could be improved to further enhance performance. System responsiveness was limited by peak motor velocity, and bandwidth could be doubled with a higher-voltage power supply. Torque control could also be improved with more sophisticated low-level programming than the proportional control scheme used here. Tests of friction characteristics have shown significant stick-slip dynamics within the Bowden cable, a source of torque error, and lower-friction conduit would improve tracking. Prosthesis end-effector mass could be further reduced by elimination of the force-amplifying pulley, which appears not to be necessary following tests of maximum Bowden-cable load. Under higher loads, the Bowden cable itself might exhibit sufficient series compliance, allowing incrementally-lighter toe structures. We are presently designing a higher-load prosthesis end-effector that would accommodate larger subjects, and a prosthesis with separate inversion-eversion torque control to impact lateral motions as well as the (dominant) sagittal motions addressed here. More human-like center of pressure progression and greater comfort might be achieved by refinements to the curvature of the passive heel element.

V. Conclusion

We have developed an experimental platform that uniquely enables rapid assessment of human response to proposed robotic ankle-foot prosthesis designs. Our results suggest that platforms of this type will enable rigorous human-subject experiments with the flexibility to evaluate a wide range of parameters and behaviors without laborious tuning of overly-specialized devices. This technology could become the core of a new experiment-centered approach to the development of biomechatronic devices, in which design requirements and trade-offs are established prior to product design tasks such as miniaturization. Such an approach could be used to address emerging scientific topics in active prosthetics and orthotics, such as dynamic stability, co-adaptation, and identification of human coordination goals.

ACKNOWLEDGMENT

We thank Soongeun Cha for design improvements, Myunghee Kim and Rachel W. Jackson for software contributions, and Peter G. Adamczyk for concepts on testbeds.

[1] K. Ziegler-Graham *et al.*, "Estimating the prevalence of limb loss in the united states: 2005 to 2050," *Arch. Phys. Med. Rehab.*, vol. 89, pp. 422–429, 2008.

[2] M. D. Hoffman *et al.*, "Physiological comparison of walking among bilateral above-knee amputee and able-bodied subjects, and a model to account for the differences in metabolic cost," *Arch. Phys. Med. Rehab.*, vol. 78, pp. 385–392, 1997.

[3] R. L. Waters and S. Mulroy, "The energy expenditure of normal and pathologic gait." *Gait Post.*, vol. 9, pp. 207–231, 1999.

[4] S. K. Au, J. Weber, and H. Herr, "Biomechanical design of a powered ankle-foot prosthesis," in *Proc. Int. Conf. Rehab. Rob.*, 2007, pp. 298–303.

[5] J. Hitt *et al.*, "Self-contained powered knee and ankle prosthesis: Initial evaluation on a transfemoral amputee," in *Proc. Int. Conf. Rehab. Rob.*, 2007, pp. 638–644.

[6] F. Sup *et al.*, "Self-contained powered knee and ankle prosthesis: Initial evaluation on a transfemoral amputee," in *Proc. Int. Conf. Rehab. Rob.*, 2009, pp. 638–644.

[7] S. H. Collins and A. D. Kuo, "Recycling energy to restore impaired ankle function during human walking," *PLoS: ONE*, vol. 5, p. e9307, 2010.

[8] A. D. Segal *et al.*, "The effects of a controlled energy storage and return prototype prosthetic foot on transtibial amputee ambulation," *Hum. Mov. Sci.*, vol. in press, 2012.

[9] K. E. Zelik *et al.*, "Systematic variation of prosthetic foot parameter affects center-of-mass mechanics and metabolic cost during walking," *Trans. Neural Syst. Rehabil. Eng.*, vol. 19, pp. 411–419, 2011.

[10] D. C. Morgenroth *et al.*, "The effect of prosthetic foot push-off on mechanical loading associated with knee osteoarthritis in lower extremity amputees," *Gait Post.*, vol. 34, pp. 502–507, 2012.

[11] H. M. Herr and A. M. Grabowski, "Bionic ankle-foot prosthesis normalizes walking gait for persons with leg amputation," *Proc. Roy. Soc. Lon. B*, vol. 279, pp. 457–464, 2012.

[12] G. S. Sawicki and D. P. Ferris, "Mechanics and energetics of level walking with powered ankle exoskeletons," *J. Exp. Biol.*, vol. 211, pp. 1402–1413, 2008.

[13] J. F. Veneman *et al.*, "Design and evaluation of the LOPES exoskeleton robot for interactive gait rehabilitation," *Trans. Neural Syst. Rehabil. Eng.*, vol. 15, pp. 379–386, 2007.

[14] W. C. Flowers and R. W. Mann, "An electrohydraulic knee-torque controller for a prosthesis simulator," *J. Biomech. Eng.*, vol. 99, pp. 3–9, 1977.

[15] J. Hidler *et al.*, "Multicenter randomized clinical trial evaluating the effectiveness of the Lokomat in subacute stroke," *Neurorehab. Neur. Rep.*, vol. 23, pp. 5–13, 2009.

[16] M. Whittle, *Gait Analysis: An Introduction*. Oxford: Butterworth-Heinemann Medical, 1996.

[17] G. Pratt and M. Williamson, "Series elastic actuators," in *Proc. Int. Conf. Intel. Rob. Sys.*, 1995.

[18] G. Wyeth, "Control issues for velocity sourced series elastic actuators," in *Proc. Aus. Conf. Rob. Autom.*, Aukland, Australia, 2006.

[19] D. A. Winter, *Biomechanics and Motor Control of Human Movement*, 2nd ed. Toronto, Canada: John Wiley & Sons, Inc., 1990.

[20] C. L. Johnson and E. L. Robinson, "Able-bodied artificial foot prosthesis testing apparatus," Patent.

[21] P. G. Adamczyk, S. H. Collins, and A. D. Kuo, "The advantages of a rolling foot in human walking," *J. Exp. Biol.*, vol. 209, pp. 3953–3962, 2006.

[22] A. Roy *et al.*, "Robot-aided neurorehabilitation: a novel robot for ankle rehabilitation," *Trans. Rob.*, vol. 25, pp. 569–582, 2009.

[23] R. C. Browning *et al.*, "The effects of adding mass to the legs on the energetics and biomechanics of walking," *Med. Sci. Sports Exer.*, vol. 39, pp. 515–525, 2007.

[24] K. E. Gordon, G. S. Sawicki, and D. P. Ferris, "Mechanical performance of artificial pneumatic muscles to power an ankle-foot orthosis," *J. Biomech.*, vol. 39, pp. 1832–1841, 2006.

[25] J. Hitt *et al.*, "Robotic transtibital prosthesis with biomechanical energy regeneration," *Indust. Rob: Int. J.*, vol. 36, pp. 441–447, 2009.

[26] G. C. Agarwal and G. L. Gottlieb, "Oscillation of the human ankle joint in response to applied sinusoidal torque on the foot," *J Physiol.*, vol. 268, pp. 151–176, 1977.

[27] J. E. Pratt *et al.*, "The roboknee: an exoskeleton for enhancing strength and endurance during walking," in *Proc. Int. Conf. Rob. Autom.*, New Orleans, LA, 2004, pp. 2430–2435.

[28] M. Noël *et al.*, "An electrohydraulic actuated ankle foot orthosis to generate force fields and to test proprioceptive reflexes during human walking," *Trans. Neural Syst. Rehabil. Eng.*, vol. 16, pp. 390–399, 2008.

[29] J. S. Sulzer *et al.*, "A highly backdrivable, lightweight knee actuator for investigating gait in stroke," *Trans. Rob.*, vol. 25, pp. 539–548, 2009.

[30] A. H. A. Stienen *et al.*, "Design of a rotational hydroelastic actuator for a powered exoskeleton for upper limb rehabilitation," *Trans. Biomed. Eng.*, vol. 57, pp. 728–735, 2010.

[31] J. Pratt, B. Krupp, and C. Morse, "Series elastic actuators for high fidelity force control," *Indust. Rob: Int. J.*, vol. 29, pp. 234–241, 2002.

[32] A. Schiele, "Performance difference of bowden cable relocated and non-relocated master actuators in virtual environment applications," in *Proc. Int. Conf. Intel. Rob. Sys.*, 2008, pp. 3507–3512.